Multi-Point Impedance Control for Redundant Manipulators

Toshio Tsuji, Achmad Jazidie, and Makoto Kaneko, *Member, IEEE*

Reprinted from
IEEE TRANSACTIONS ON SYSTEMS, MAN, AND CYBERNETICS—PART B: CYBERNETICS
Vol. 26, No. 5, October 1996

Multi-Point Impedance Control for Redundant Manipulators

Toshio Tsuji, Achmad Jazidie, and Makoto Kaneko, *Member, IEEE*

Abstract—**The present paper proposes an impedance control method called the Multi-Point Impedance Control (MPIC) for redundant manipulators. The method can not only control end-effector impedance, but also regulate impedances of several points on the links of the manipulator, which are called virtual end-point impedances, utilizing arm redundancy. Two approaches for realizing the MPIC are presented. In the first approach, controlling the end-effector impedance and the virtual end-point impedances are considered as the tasks with the same level, and the joint control law developed in this approach can realize the closest impedances of the multiple points, including the end-effector and the virtual end-points to the desired ones in the least squared sense. On the other hand, in the second approach, controlling the end-effector impedance is considered the most important task, and regulating the impedances of the virtual end-points is considered as a sub-task. Under the second approach, the desired end-effector impedance can be always realized since the joint control torque for the regulation of the virtual end-point impedances is designed in such a way that it has no effect on the end-effector motion of the manipulator. Simulation experiments are performed to confirm the validity and to show the advantages of the proposed method.**

I. Introduction

REDUNDANCY occurs when a robot possesses extra degrees of freedom to execute a given task. This is a desirable feature that may lead to more dexterity and versatility of robot motions. Research activities focused on resolution of the redundancy have been increased, in particular, concerning the inverse kinematics, in terms of how to determine a manipulator configuration that is constrained to follow a specified end-effector trajectory while optimizing various secondary criteria such as singularity avoidance, obstacle avoidance, and various measures of dexterity [1]–[7]. On the other hand, redundancy on a force/torque transformation has been pointed out by [8] and [9]. Khatib pioneered the use of the null space on the force/torque transformation to control the internal motion of the redundant manipulator [8]. Kang and Freeman [9] derived the null space damping method for several performance criteria. Also, using the concept of dynamic redundant degrees of freedom, Arai *et al.* [10] has proposed a method to utilize the force redundancy for minimizing the joint torque.

Manuscript received July 10, 1994; revised July 25, 1995.

T. Tsuji and M. Kaneko are with Computer Science and Systems Engineering, Faculty of Engineering, Hiroshima University, Higashi-Hiroshima, 739 Japan (e-mail: tsuji@huis.hiroshima-u.ac.jp).

A. Jazidie is with Control Systems Engineering Laboratory, Surabaya Institute of Technology, Sukolilo-Surabaya, 60111 Indonesia.

Publisher Item Identifier S 1083-4419(96)05356-3.

When a robot performs a task that requires mechanical interactions with an environment or an object being manipulated, the robot has to develop a compliant motion in which the interaction force along the constrained direction should be controlled properly, so that the manipulator complies with the environmental constraints. Impedance control [11] is one of the most effective methods for the development of such compliant motion. This method has many desirable attributes such as an ability to come into contact with a hard surface without losing stability and an ability to specify directly the behavior of the mechanical interaction with the environment. The effectiveness and the robustness of the impedance control has been discussed and demonstrated in detail elsewhere by several researchers [12]–[16].

Up to the present, however, a few studies such as [17] by Newman and Dohring and [18] by Peng and Adachi have been reported utilizing kinematic redundancy in terms of impedance control using the extended Jacobian scheme proposed in [6]. In this scheme, a vector of new task variables is defined, the dimension of which is equal to the number of degrees of freedom of kinematic redundancy. This additional output vector is augmented to the end-effector position vector to make a corresponding Jacobian matrix square. Then, based on the augmented Jacobian matrix, an impedance control law was derived to achieve the desired end-effector impedance as well as to satisfy the secondary constraint. In [17], however, controlling end-effector inertia has not been taken into account. So, in fact, this method reduces to the active stiffness control [19]. On the other hand, in order to guarantee that the augmented Jacobian is always of full rank, Peng and Adachi in [18] have introduced a differentiable scalar objective function as a function of joint angles, the gradient of which is projected onto the null space of the end-effector Jacobian matrix. This leads to a control strategy that provides an impedance control for the end-effector as well as satisfies the optimal condition of the objective function.

In this paper, an impedance control method called the Multi-Point Impedance Control (MPIC) for redundant manipulators, which has been originally proposed in terms of the compliance control [20] and developed in [21], is illustrated in a unified way. The proposed method can regulate the impedances of several points on the links of the manipulator while controlling the end-effector impedance. In regards to the way of realizing the desired multiple point impedances, two approaches in the development of the MPIC are presented.

In the first approach, the desired end-effector impedance and the desired impedances of several points are concatenated to

form a new desired impedance matrix that we want to realize. Implicitly, it means that controlling the end-effector impedance and the impedances of several points are considered as the tasks with the same level of importance. Then, the multi-point impedance control law is developed in terms of how to specify joint impedance matrices in order to achieve the desired multiple point impedances. Generally, the manipulator loses redundant joint degrees of freedom as the number of points that we want to regulate their impedances is increased, and finally it becomes over-constrained. The proposed method can give the optimal solution for both the redundant and over-constrained cases in the least squared sense.

In the second approach, the control law is developed based on the Hierarchical Impedance Control (HIC) scheme proposed by Jazidie *et al.* [22]. The HIC scheme is a framework that has been developed in order to utilize the redundancy in the force/torque relationship in terms of impedance control. It can control not only end-effector impedance using one of the conventional impedance control methods, but also regulate additional arm impedance. The HIC scheme has been introduced by incorporating an additional controller to the end-effector impedance controller in such a way that the additional controller has no effect on the dynamic behavior of the end-effector motion. As a result, under the second approach, the desired end-effector impedance can always be realized, since controlling the end-effector impedance is considered as the most important task and regulating the other several point impedances as a sub-task.

The MPIC presented here is useful for certain environments where some objects exist on the task space of the manipulator. For example, when the manipulator close to the objects performs a task that requires the end-effector compliant motion, it is worth controlling the impedances of several points on the links of the manipulator in order to avoid a collision with them as well as regulating the end-effector impedance for the task. In this case, first the closest point on the manipulator to the object is defined as a virtual end-point. Then, the impedance of the virtual end-point is regulated to be stiff in the direction of the object in order to avoid a collision caused by unexpected external forces to the manipulator in addition to controlling the impedance of the end-effector. On the other hand, if the virtual end-points are required to interact with the objects, then the impedances of the virtual end-points are regulated in order to accommodate to an interaction force so as to comply with environmental constraints imposed by the objects. Also, the proposed method can be easily applied to a macro-/mini-manipulator system. By incorporating a lightweight mini-manipulator into a standard manipulator (the macro-manipulator), the capability of the manipulator system to perform fine motions can be significantly improved [23], [24]. Using the MPIC, we can control the end-effector impedance of the macro-manipulator and/or the coupling impedance between the end-effectors of the mini- and the macro-manipulators while controlling the end-effector impedance of the mini-manipulator.

The paper is organized as follows: Section II is devoted to give an illustration of a manipulator performing a task close to obstacles, and the definition and kinematic structure of the virtual arm corresponding to the virtual end-point are given. Then, based on the concept of the virtual arm, two approaches of the multi-point impedance control law are presented in Sections III and IV, respectively. Finally, the effectiveness of the proposed method is shown by simulation experiments in Section V.

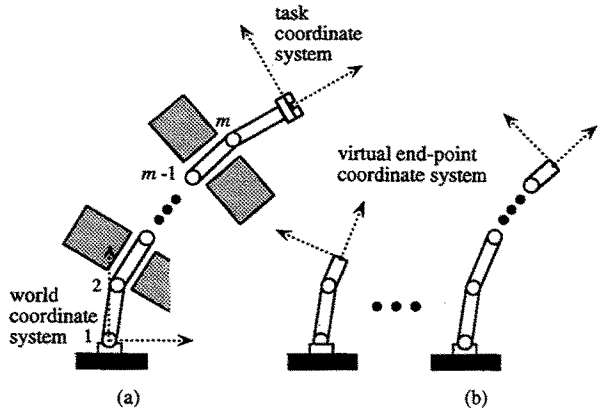

Fig. 1. Manipulator close to obstacles: (a) actual arm and the obstacles, and (b) virtual arms.

II. Virtual Arm and its Kinematics

A. Virtual Arm

We consider a redundant manipulator having m joints shown in Fig. 1(a). Since the manipulator performing a task that requires compliant motion of the end-point is close to some obstacles, the manipulator may collide with them due to unexpected disturbance force. Then, as shown in Fig. 1(b), a virtual arm is defined as an arm that has its end-effector (hereafter, referred as a *virtual end-point*) located on a joint or a link of the actual arm [20], [25]. Using the virtual arms, the interaction between the manipulator and its environment can be considered within the framework of the impedance control. For example, to avoid a collision with the obstacle due to disturbance forces, the impedances of the virtual end-points should be as large (stiff) as possible in the direction of the obstacles. Also, to comply with environmental constraints imposed by the objects, the impedances of the virtual end-points should be regulated small (compliant). Here, n_v virtual arms are generally considered corresponding to the number of the virtual end-points.

B. Kinematics of the Virtual Arm

Let the virtual end-point position and velocity vectors of the i-th virtual arm in the i-th virtual end-point coordinate system be denoted as $X_{vi} \in \Re^l$ and $\dot{X}_{vi} \in \Re^l$, respectively. Let also the corresponding force vector and joint torque vector be denoted as $F_{vi} \in \Re^l$ and $\tau \in \Re^m$, respectively. For redundant manipulators, m is larger than l. The instantaneous forward kinematics of the i-th virtual arm is given by

$$\dot{X}_{vi} = J_{vi}\dot{\theta} \tag{1}$$

$$\tau = J_{vi}^T F_{vi} \tag{2}$$

where $J_{vi} \in \Re^{l \times m}$ is the Jacobian matrix associated with the i-th virtual arm. Concatenating (1) and (2) for all virtual arms, we can obtain the instantaneous kinematics as given by

$$\dot{X}_v = J_v \dot{\theta} \tag{3}$$

$$\tau = J_v^T F_v \tag{4}$$

where $\dot{X}_v = [\dot{X}_{v1}^T \dot{X}_{v2}^T \cdots \dot{X}_{vn_v}^T]^T \in \Re^{n_v l}$ and $F_v = [F_{v1}^T F_{v2}^T \cdots F_{vn_v}^T]^T \in \Re^{n_v l}$ are the concatenated end-point velocity vector and the concatenated force vector of all virtual end-points, respectively. $J_v = [J_{v1}^T J_{v2}^T \cdots J_{vn_v}^T]^T \in \Re^{n_v l \times m}$ is the concatenated Jacobian matrix of the virtual arms. In the following sections, two approaches of the multi-point impedance control are developed using the concept of the virtual arms.

III. Multi-Point Impedance Control: First Approach

A. Relationships Between Joint Impedance and Multi-Point Impedance

When the manipulator interacts with the environment not only through the actual end-effector but also through the virtual end-points, the motion equation of the manipulator can be written in the following form:

$$M(\theta)\ddot{\theta} + h(\theta, \dot{\theta}) = \tau + J_e^T F_e^{\text{ext}} + J_v^T F_v^{\text{ext}} \tag{5}$$

where $F_v^{\text{ext}} \in \Re^{n_v l}$ is the concatenated external force vector exerted on the virtual end-points; $F_e^{\text{ext}} \in \Re^l$ is the external force exerted on the end-effector; $\theta \in \Re^m$ is the joint angle vector; $M(\theta) \in \Re^{m \times m}$ is the nonsingular inertia matrix (hereafter denoted by M); $h(\theta, \dot{\theta}) \in \Re^m$ is the nonlinear term representing the joint torque vector due to the centrifugal, Coriolis, gravity and friction forces; $\tau \in \Re^m$ is the joint control torque vector; and $J_e \in \Re^{l \times m}$ is the end-effector Jacobian matrix.

The target impedances of the end-effector and the virtual end-points are, respectively, expressed by

$$M_e d\ddot{X}_e + B_e d\dot{X}_e + K_e dX_e = F_e^{\text{ext}} \tag{6}$$

$$M_v d\ddot{X}_v + B_v d\dot{X}_v + K_v dX_v = F_v^{\text{ext}} \tag{7}$$

where M_e, B_e, $K_e \in \Re^{l \times l}$ are the desired inertia, viscosity and stiffness matrices of the end-effector, respectively; and $dX_e = X_e - X_e^d \in \Re^l$ is the deviation vector of the end-effector position from the desired trajectory X_e^d. On the other hand, M_v, B_v, $K_v \in \Re^{n_v l \times n_v l}$ are the concatenated desired inertia, viscosity and stiffness matrices of the virtual end-points, respectively; and $dX_v = X_v - X_v^d \in \Re^{n_v l}$ is the concatenated deviation vector of the virtual end-points from its desired trajectory $X_v^d \in \Re^{n_v l}$.

Let us define $J_c = [J_v^T J_e^T]^T \in \Re^{(n_v+1)l \times m}$ as the concatenated Jacobian matrix for all virtual arms and the actual arm. Using the concatenated Jacobian matrix, J_c, the motion equation of the manipulator (5) can be rewritten in the form

$$M(\theta)\ddot{\theta} + h(\theta, \dot{\theta}) = \tau + J_c^T F_c^{\text{ext}} \tag{8}$$

where $F_c^{\text{ext}} = [(F_v^{\text{ext}})^T \ (F_e^{\text{ext}})^T]^T \in \Re^{(n_v+1)l}$ is the concatenated external force vector exerted on the virtual end-points and the end-effector.

Now, (6) and (7) are concatenated to express a new target impedance as given by

$$M_c d\ddot{X}_c + B_c d\dot{X}_c + K_c dX_c = F_c^{\text{ext}} \tag{9}$$

where M_c, B_c, $K_c \in \Re^{(n_v+1)l \times (n_v+1)l}$ are the concatenated desired inertia, viscosity and stiffness matrices of the end-effector and the virtual end-points, respectively, and $dX_c = [(dX_v)^T (dX_e)^T]^T \in \Re^{(n_v+1)l}$ is the concatenated deviation vector of all end-points from the concatenated desired trajectory, $X_c^d = [(X_v^d)^T (X_e^d)^T]^T \in \Re^{(n_v+1)l}$.

Then the control law is given by

$$\tau = \tau_{\text{imp}} + \tau_{\text{comp}} \tag{10}$$

where $\tau_{\text{imp}} \in \Re^m$ is the joint torque vector needed to produce the desired multi-point impedance; and $\tau_{\text{comp}} \in \Re^m$ is the joint torque vector for the nonlinear compensation.

The term $\tau_{\text{imp}} \in \Re^m$ is defined as

$$\tau_{\text{imp}} = -M_j d\ddot{\theta} - B_j d\dot{\theta} - K_j d\theta + M\ddot{\theta} - J_c^T M_c \dot{J}_c \dot{\theta} \tag{11}$$

where M_j, B_j, $K_j \in \Re^{m \times m}$ are the inertia, viscosity, and stiffness matrices of the joint, respectively; and $d\theta = \theta - \theta^d \in \Re^m$ is the deviation vector of the joint position from the desired trajectory θ^d. On the other hand, the nonlinear compensation in the joint space is used for simplicity, and given by

$$\tau_{\text{comp}} = \tilde{h}(\theta, \dot{\theta}) \tag{12}$$

where $\tilde{h}(\theta, \dot{\theta})$ may be computed using the motion equation of the manipulator with estimated link parameters [26]. It is assumed that $\tilde{h}(\theta, \dot{\theta}) = h(\theta, \dot{\theta})$ and the manipulator's configuration is not in a singular posture.

Applying the control law given in (10)–(12) to the motion equation of the manipulator (8), we can find

$$M_j d\ddot{\theta} + B_j d\dot{\theta} + K_j d\theta = J_c^T F_c^{\text{ext}} - J_c^T M_c \dot{J}_c \dot{\theta}. \tag{13}$$

Now, substituting (9) into (13) and using the kinematic relationships of all end-points including the end-effector, we finally have the following equations:

$$M_j = J_c^T M_c J_c \tag{14}$$

$$B_j = J_c^T B_c J_c \tag{15}$$

and

$$K_j = J_c^T K_c J_c. \tag{16}$$

The above equations give the relationships between the joint impedance matrices and the multi-point impedance matrices. The joint impedance matrices, M_j, B_j, K_j, which satisfy (14)–(16), may regulate the impedances of the end-effector and the virtual end-points to some extents. For a certain condition, the desired multi-point impedance can be realized exactly. In general, however, the manipulator loses the redundant joint degrees of freedom as the number of points that we want to regulate their impedances are increased, and finally it becomes over-constrained. In the following subsection, an algorithm for obtaining the optimal joint impedance parameters that can regulate the multiple point impedances as close as possible to the desired ones is developed.

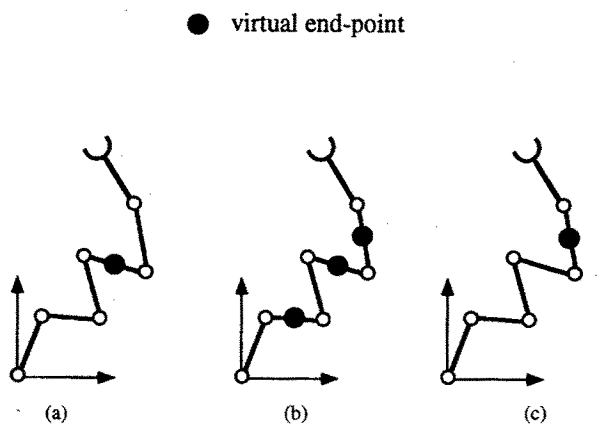

Fig. 2. Three cases of the virtual arms: (a) a redundant case, (b) an over-constrained case, and (c) a singular case.

B. Optimal Joint Impedance

Depending on the location and the number of the virtual end-points, kinematic conditions of the manipulator may occur to be under-constrained, over-constrained, or singular [20], [25]. Fig. 2 illustrates three conditions of a six-joint planar manipulator ($m = 6$) where one or more virtual end-points are located on the links of the manipulator, and only two degrees of freedom of translational motion on the task space are considered for simplicity ($l = 2$). The kinematic conditions can be categorized depending on the number and the location of the virtual end-points as follows: 1) a redundant case [Fig. 2(a)], 2) an over-constrained case [Fig. 2(b)], and 3) a singular case [Fig. 2(c)].

The rank of J_c reflects three cases mentioned above [20], [25]: J_c is of full row rank for the redundant case, of full column rank for the over-constrained case, and not of full rank for the singular case. It should be noted that a case in which J_c becomes a square matrix with full rank is considered as a special instance of the redundant cases, and it may be called a nonsingular case. Consequently, the rank of J_c determines the property of the matrix equations (14)–(16).

Let us assume that the desired multiple point impedances are given according to the task. For the redundant cases, the desired multiple point impedances can be always realized and (14)–(16) directly give the minimum norm solutions of the joint impedance matrices corresponding to the given desired multi-point impedance matrices, M_c, B_c, K_c. On the other hand, for the over-constrained and singular cases, there are no joint impedance matrices that realize the given desired multiple point impedances in general.

In the following, the general approach to obtain the optimal joint impedance matrices for all of three cases is explained using the maximum rank decomposition of the concatenated Jacobian matrix J_c

$$J_c = J_{ca} J_{cb} \tag{17}$$

where $J_{ca} \in \Re^{(n_v+1)l \times p}$ and $J_{cb} \in \Re^{p \times m}$ have the same rank as J_c: rank J_c = rank J_{ca} = rank $J_{cb} = p$. The matrices J_{ca} and J_{cb} in (17) express an over-constrained part and an under-constrained part of the concatenated Jacobian matrix J_c, respectively.

First, the optimal way to obtain the joint inertia matrix M_j is derived. By substituting (17) into (14), we have

$$M_j = J_{cb}^T J_{ca}^T M_c J_{ca} J_{cb}. \tag{18}$$

Then, (18) is divided into the following two equations:

$$M_{jb} = J_{ca}^T M_c J_{ca} \tag{19}$$

$$M_j = J_{cb}^T M_{jb} J_{cb}. \tag{20}$$

The matrix $J_{ca}^T M_c J_{ca}$ in (19) is always invertible whenever the desired concatenated inertia matrix M_c is given as a nonsingular one. Therefore, (19) can be transformed into

$$M_c^{-1} = J_{ca} M_{jb}^{-1} J_{ca}^T. \tag{21}$$

In general, since the matrix J_{ca} is of full column rank, the solution M_{jb}^{-1} that satisfies (21) does not exist. In this case, the goal is to find a matrix M_{jb}^{-1} to minimize

$$G_1\left(M_{jb}^{-1}\right) = \left\| W\left(M_c^{-1} - J_{ca} M_{jb}^{-1} J_{ca}^T\right) W^T \right\| \tag{22}$$

where $\|A\|$ stands for a matrix norm defined by

$$\|A\| = \{\mathrm{tr}(A^T A)\}^{0.5} \tag{23}$$

where $\mathrm{tr}(A^T A)$ denotes a trace of the matrix $A^T A$. The matrix $W \in \Re^{(n_v+1)l \times (n_v+1)l}$ in (22) is a nonsingular diagonal matrix that can weight the desired multiple point impedances according to the given task.

The necessary condition that the optimal solution must satisfy is

$$\partial G_1\left(M_{jb}^{-1}\right) / \partial M_{jb}^{-1} = 0. \tag{24}$$

Substituting (22) into (24) and expanding it, we can obtain

$$M_{jb}^{-1} = J_w^{\#} W M_c^{-1} W^T \left(J_w^{\#}\right)^T \tag{25}$$

$$J_w = W J_{ca} \tag{26}$$

using the partial differential formulas about the trace of a matrix [27], where $J_w^{\#}$ is defined as $J_w^{\#} \equiv (J_w^T J_w)^{-1} J_w^T$. Since the matrix $J_w^T J_w \in \Re^{p \times p}$ is always invertible and rank $J_{ca} = p$, we can obtain from (25)

$$M_{jb} = \left(J_w^T J_w\right)\left(J_w^T W M_c^{-1} W^T J_w\right)^{-1}\left(J_w^T J_w\right). \tag{27}$$

Consequently, we can get the optimal joint inertia matrix M_j using (20) and (27).

The method developed above can be applied to all the cases shown in Fig. 2. In particular, the computation is dramatically simplified in the redundant and over-constrained cases. In the redundant case, since $J_{ca} = I_{(n_v+1)l}$ (an $(n_v+1)l \times (n_v+1)l$ unit matrix) and $J_{cb} = J_c$, we can see that $M_{jb} = M_c$, and the joint inertia matrix is reduced to (14). Also, in the over-constrained cases, since $J_{ca} = J_c$ and $J_{cb} = I_m$, we can see that $M_j = M_{jb}$, and the joint inertia matrix is reduced to

$$M_j = \left(J_{wc}^T J_{wc}\right)\left(J_{wc}^T W M_c^{-1} W^T J_{wc}\right)^{-1}\left(J_{wc}^T J_{wc}\right) \tag{28}$$

$$J_{wc} = W J_c. \tag{29}$$

Using the same way as the above, we can also find the optimal solutions for the joint viscosity and stiffness matrices as given by

$$B_{jb} = \left(J_w^T J_w\right)\left(J_w^T W B_c^{-1} W^T J_w\right)^{-1}\left(J_w^T J_w\right) \quad (30)$$

$$B_j = J_{cb}^T B_{jb} J_{cb} \quad (31)$$

and

$$K_{jb} = \left(J_w^T J_w\right)\left(J_w^T W K_c^{-1} W^T J_w\right)^{-1}\left(J_w^T J_w\right) \quad (32)$$

$$K_j = J_{cb}^T K_{jb} J_{cb} \quad (33)$$

where J_w is given by (26).

It can be easily seen that the joint torque τ_{imp} in (11) can be expressed by

$$\tau_{\text{imp}} = -J_c^T(\tilde{M}_c d\ddot{X}_c + \tilde{B}_c d\dot{X}_c + \tilde{K}_c dX_c) + M\ddot{\theta} + J_c^t(\tilde{M}_c - M_c)\dot{J}_c\dot{\theta} \quad (34)$$

where $\tilde{M}_c$, $\tilde{B}_c$, and $\tilde{K}_c$ are, respectively, given by

$$\tilde{M}_c = \left(J_c^T\right)^+ M_j J_c^+ \quad (35)$$

$$\tilde{B}_c = \left(J_c^T\right)^+ B_j J_c^+ \quad (36)$$

$$\tilde{K}_c = \left(J_c^T\right)^+ K_j J_c^+ \quad (37)$$

The optimal joint impedance matrices, M_j, B_j, and K_j, obtained here give the realized concatenated multi-point impedance matrices, $\tilde{M}_c$, $\tilde{B}_c$, and $\tilde{K}_c$, which are closest to the desired concatenated multi-point impedance matrices, M_c, B_c, and K_c, in terms of the cost function (22). It should be noted that for the redundant case, the joint torque τ_{imp} can be computed directly from the desired concatenated multi-point impedance matrices M_c, B_c, and K_c as given by

$$\tau_{\text{imp}} = -J_c^T(M_c d\ddot{X}_c + B_c d\dot{X}_c + K_c dX_c) + M\ddot{\theta} \quad (38)$$

since the matrices M_c, B_c, and K_c can be always realized exactly.

In summary, the first approach provides a compact formulation for controlling the multiple point impedances of redundant manipulators. It can be seen that in the redundant case, this approach can realize the given desired multiple point impedances exactly and the computation is relatively simple. However, in the over-constrained and singular cases, a problem will arise for the tasks where the compliant motion of the end-effector is critically significant, since exact realization of the end-effector impedance is not guaranteed. Next, on the basis of the HIC scheme [22], the development of the second approach is presented in the following section.

IV. Multi-Point Impedance Control: Second Approach

A. Hierarchical Impedance Control (HIC)

Sufficient Condition of the HIC Scheme: The basic idea and the sufficient condition of the HIC scheme [22] is briefly described in this section. First, let us consider an m-joint redundant manipulator that interacts with the environment only through its end-effector. The motion equation of the manipulator is expressed by

$$M(\theta)\ddot{\theta} + h(\theta, \dot{\theta}) = \tau + J^T F_e^{\text{ext}}. \quad (39)$$

The target impedance of the end-effector is given in (6). In the hierarchical impedance control scheme, the control law is given by

$$\tau = \tau_{\text{effector}} + \tau_{\text{comp}} + \tau_{\text{add}} \quad (40)$$

where $\tau_{\text{effector}} \in \Re^m$ is the joint torque vector required to produce the desired end-effector impedance; and $\tau_{\text{add}} \in \Re^m$ is the joint torque vector for a sub-task. For the term $\tau_{\text{effector}} \in \Re^m$, the impedance control law without calculation of inverse Jacobian matrix [12] is adopted

$$\tau_{\text{effector}} = J_e^T\left[\Lambda\left\{\ddot{X}^d - M_e^{-1}(B_e d\dot{X}_e + K_e dX_e) - \dot{J}_e\dot{\theta}\right\} - \left\{I_l - \Lambda M_e^{-1}\right\}F_e^{\text{ext}}\right] \quad (41)$$

where I_1 is an $l \times l$ unit matrix; and $\Lambda = (J_e M^{-1} J_e^T)^{-1} \in \Re^{l\times l}$ is defined as the operational space kinetic energy matrix [28]. Also, the nonlinear compensation in the joint space is used for simplicity and given as in (12).

If the additional joint control torque, τ_{add}, satisfies the following condition:

$$\bar{J}_e^T \tau_{\text{add}} = 0 \quad (42)$$

where $\bar{J}_e = M^{-1} J_e^T \Lambda \in \Re^{m\times l}$, then τ_{add} dynamically has no effect to the end-effector motion of the manipulator, and the end-effector impedance remains equal to the target impedance given in (6) (see Appendix A).

Optimal Additional Controller: Kang and Freeman [9] derived the general solution of (42) using three kinds of local joint torque optimization schemes: joint torque minimization, natural joint motion and joint acceleration minimization. Note that the null space derived by natural joint motion and joint torque minimization criteria are the same as the ones proposed by Khatib [8] and Jazidie *et al.* [22], respectively.

In the present paper, using the natural joint motion criterion, we will derive the additional optimal controller, τ_{add}, corresponding to the desired joint torque, τ_{add}^*. First, the null space derived by the natural joint motion criterion is given by

$$\tau_{\text{add}} = \left(I_m - J_e^T \bar{J}_e^T\right) z \quad (43)$$

where I_m is an $m \times m$ unit matrix, and $z \in \Re^m$ is an arbitrary vector. The joint torque, τ_{add}, in (43) always satisfies the sufficient condition (42), and now the problem becomes how to find the arbitrary vector z in (43) to minimize the following cost function: $G_2(\tau_{\text{add}})$

$$G_2(\tau_{\text{add}}) = (\tau_{\text{add}}^* - \tau_{\text{add}})^T M^{-1}(\tau_{\text{add}}^* - \tau_{\text{add}}). \quad (44)$$

The cost function (44) describes the inertia inverse weighted driving force or the acceleration energy about the discrepancy between τ_{add} and τ_{add}^* [8]. Using the least square method, we can find the optimal solution (see Appendix B) as given by

$$\tau_{\text{add}} = \left(I_m - J_e^T \bar{J}_e^T\right)\tau_{\text{add}}^*. \quad (45)$$

The joint torque of (45) is the optimal one corresponding to the cost function (44) and has no effect on the dynamic behavior of the end-effector motion, since τ_{add} always lies in the null space of $\bar{J}_e^T$. As a result, under the HIC, it is possible to utilize arm redundancy through a suitable selection of the

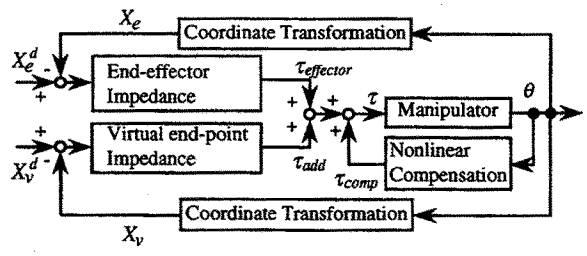

Fig. 3. Block diagram of the second approach of the MPIC. The method can control the virtual end-point impedances as well as the end-effector impedance of the redundant manipulator.

additional controller, τ_{add}, in the sense that the manipulator can perform a sub-task while controlling the end-effector impedance.

B. Derivation of the Control Law

Now, we will derive the multi-point impedance control law based on the HIC scheme. Instead of (40), the joint control torque is given by

$$\tau = \tau_{\text{effector}} + \tau_{\text{comp}} + \tau_{\text{add}} - (\bar{J}_e J_e)^T J_v^T F_v^{\text{ext}} \tag{46}$$

including the cancellation torque, $(\bar{J}_e J_e)^T J_v^T F_v^{\text{ext}}$, for the effects of the external forces exerted on the virtual end-points to the actual end-effector motion.

The concatenated target impedance for the virtual end-points is given in (7). In order to determine the desired joint torque, τ_{add}^*, for controlling the virtual end-point impedances, the effects of τ_{add}^* to the actual end-effector impedance is ignored as the first step, i.e., the null space transformation matrix is assumed to be an identity matrix in (45), and τ_{add} in (46) is reduced to τ_{add}^*. Then, based on the force/torque relationship (4) of the virtual arms, we can find the following joint torque for controlling the virtual end-point impedances:

$$\begin{aligned}\tau_{\text{add}}^* = &-J_v^T(M_v d\ddot{X}_v + B_v d\dot{X}_v + K_v dX_v) \\ &- \tau_{\text{effector}} + (\bar{J}_e J_e)^T J_v^T F_v^{\text{ext}} - J_e^T F_e^{\text{ext}} + M\ddot{\theta}.\end{aligned} \tag{47}$$

Under the HIC framework, the coupling effects of τ_{add}^* to the actual end-effector impedance can be filtered out through the null space transformation matrix using equation (45), and the additional joint control torque τ_{add} is assured to be always the optimal one corresponding to the cost function (44). Therefore, substituting (47) into (45) we have

$$\begin{aligned}\tau_{\text{add}} = &-(I_m - J_e^T \bar{J}_e^T) J_v^T (M_v d\ddot{X}_v + B_v d\dot{X}_v + K_v dX_v) \\ &+ (I_m - J_e^T \bar{J}_e^T) M\ddot{\theta}\end{aligned} \tag{48}$$

using the following property:

$$(I_m - J_e^T \bar{J}_e^T) J_e^T u = 0 \tag{49}$$

where $u \in \Re^l$ is an arbitrary vector. The block diagram of the hierarchical multi-point impedance control developed in this section is shown in Fig. 3.

C. Validity of the Control Law

It has been shown that there are three kinematic conditions depending on the number and the location of the virtual end-points, which are reflected by the rank of the concatenated Jacobian matrix J_C (see Sect III-B). These cases are examined in terms of the MPIC derived in the previous subsection.

Applying the MPIC [(12), (41), (46), and (48)] to the motion equation of the manipulator (5), we can have the following equation:

$$(I_m - J_e^T \bar{J}_e^T) J_v^T (M_v d\ddot{X}_v + B_v d\dot{X}_v + K_v dX_v - F_v^{\text{ext}}) = 0. \tag{50}$$

It can be seen that the realization of the virtual end-point impedances depends on the rank of the matrix $(I_m - J_e^T \bar{J}_e^T) J_v^T$. When the matrix $(I_m - J_e^T \bar{J}_e^T) J_v^T$ is of full column rank, the concatenated target impedance of the virtual end-points (7) can be realized exactly. Otherwise, the impedances of the virtual end-points may differ from the desired ones.

Here, we can introduce the following theorem on the relationship between the rank of $(I_m - J_e^T \bar{J}_e^T) J_v^T$ and the rank of the concatenated Jacobian matrix J_c [29] and [30]:

Theorem 1: When the end-effector Jacobian matrix J_c is of full row rank matrix, then the matrix $(I_m - J_e^T \bar{J}_e^T) J_v^T$ is of full column rank if and only if the concatenated Jacobian matrix J_c is of full row rank.

This means that the realization of the virtual end-point impedances is reduced to the rank of the concatenated Jacobian matrix J_c, which is consistent with the kinematic conditions of the virtual arms discussed in Sect. III-B.

Summing up, the second approach considers controlling the end-effector impedance as the most important task, and the additional joint torque for the regulation of the virtual end-point impedances is designed in such a way that it has no effect on the end-effector motion. Therefore, under the second approach, the desired end-effector impedance can be always realized. It should be noted that in the redundant cases [Fig. 2(a)], the desired multiple point impedances can be realized simultaneously under the second approach. On the other hand, in the over-constrained and singular cases, the end-effector impedance can be controlled exactly while the virtual end-point motions are expected to be strongly reflected by their target impedances.

V. Simulation Experiments

The effectiveness of the proposed method is verified by computer simulations using planar manipulators where the dimension of the task space includes two translations and one rotation ($l = 3$). The first set of simulation experiments is intended to evaluate the dynamic response of the six-joint manipulator ($m = 6$) under the proposed method where the disturbance forces, $F_e^{\text{ext}} = [-2\ (\text{N}),\ -2\ (\text{N}),\ 2\ (\text{Nm})]^T$, and $F_v^{\text{ext}} = [-2\ (\text{N}),\ 2\ (\text{N}),\ 2\ (\text{Nm})]^T$, are exerted to the end-effector and the virtual end-point, respectively. The simulations are performed for a nonsingular case, where the virtual end-point was located on the middle point of the third link $n_v = 1$ (see Fig. 4). The link parameters of the manipulator are shown in Table I.

TABLE I
LINK PARAMETERS OF THE SIX-JOINT PLANAR MANIPULATOR

	link i $(i = 1, \ldots, 6)$
length (m)	0.4
mass (kg)	3.0
center of mass (m)	0.2
moment of inertia kgm $(^2)$	0.32

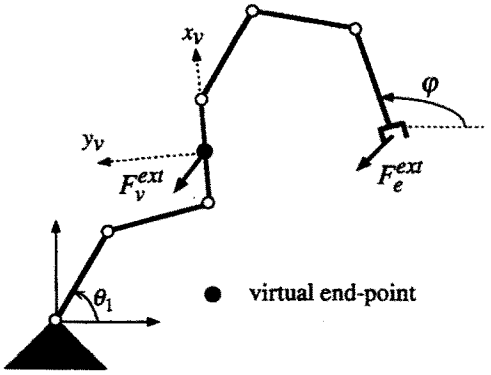

$\theta = [\ 1.0, -0.8, 1.4, -0.6, -1.2, -1.0\ ]^T$ (rad)

Fig. 4. Model of a six-joint planar manipulator.

Fig. 5 shows the simulation results under the conventional impedance control [11], where Fig. 5(a) and (b) indicates the change of manipulator posture and the time history of the end-effector position, respectively. On the other hand, Figs. 6 and 7 show the motion profile of the manipulator under the first and the second approaches of the MPIC, respectively. Equation (38) was used in the simulation using the first approach.

The desired end-effector impedance matrices were set as M_e = diag. [0.4 (kg), 0.25 (kg), 0.4 (kgm^2)], B_e = diag. [2 (N/(m/s)), 2.5 (N/(m/s)), 4 (Nm/(rad/s))], K_e = diag. [10 (N/m), 100 (N/m), 10 (Nm/rad)]. Also, in Figs. 6 and 7, the desired virtual end-point impedance matrices were set as M_v = diag. [0.4 (kg), 0.25 (kg), 0.4 (kgm^2)], B_v, = diag. [2 (N/(m/s)), 2.5 (N/(m/s)), 4 (Nm/(rad/s))], K_v = diag. [10 (N/m), 100 (N/m), 10 (Nm/rad)]. Under these impedance matrices, the damping ratios of the desired dynamic behavior in the directions of x, y axes and the rotation become equal to 0.5, 0.25, and 1.0, respectively, for both the end-effector and the virtual end-point. On the other hand, the settling times for all directions of the end-effector and the virtual end-point become equal to 0.8 s. Also, the desired end-effector's and virtual end-point's trajectories are set as $X_e^d(t) = X_e(0)$, and $X_v^d(t) = X_v(0)$, respectively. The computations of the manipulator dynamics were performed by the Appel's method [31]. It should be noted that in the simulations using conventional impedance control, a dissipative joint torque was added to the controller in order to avoid the undamped internal joint motion of the redundant manipulator as follows:

$$\tau_{\text{dissp}} = -d\left(I_m - J_e^T \bar{J}_e^T\right)\dot{\theta} \tag{51}$$

where d is a positive scalar constant and it was set equal to 10 (Nm/(rad/s)). The above dissipative joint torque has no effect to the end-effector motion. Also, the cancellation torque for

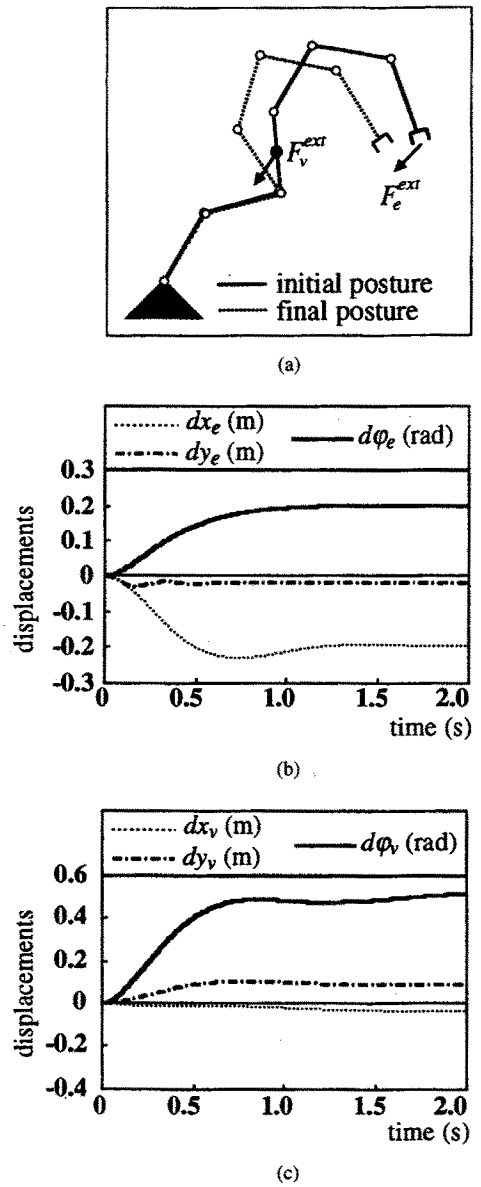

Fig. 5. Motion profile of the six-joint manipulator for external force under the conventional impedance control: (a) stick pictures, (b) end-effector displacements, and (c) displacements of the middle point of the third link.

the effects of the external force exerted on the virtual end-point was included in the conventional impedance controller in order to realize the desired end-effector impedance.

The response of the end-effeçtors in Figs. 5–7 are exactly the same, where the realized end-effector motion is completely reflected by the desired impedance. In terms of the virtual end-point, however, the difference between the conventional impedance control and the proposed methods appears clearly. In Figs. 6 and 7, since the virtual end-point was located on the middle point of the third link, there are enough degrees of the freedom to realize the desired impedances of both the end-effector and the virtual end-point simultaneously. In this case, the concatenated Jacobian J_c is of square and full rank, and the rank of $(I_m - J_e^T \bar{J}_e^T) J_v^T \in \Re^{6\times 3}$ is equal to 3. It can be seen from Figs. 6(c) and 7(c) that the dynamic responses

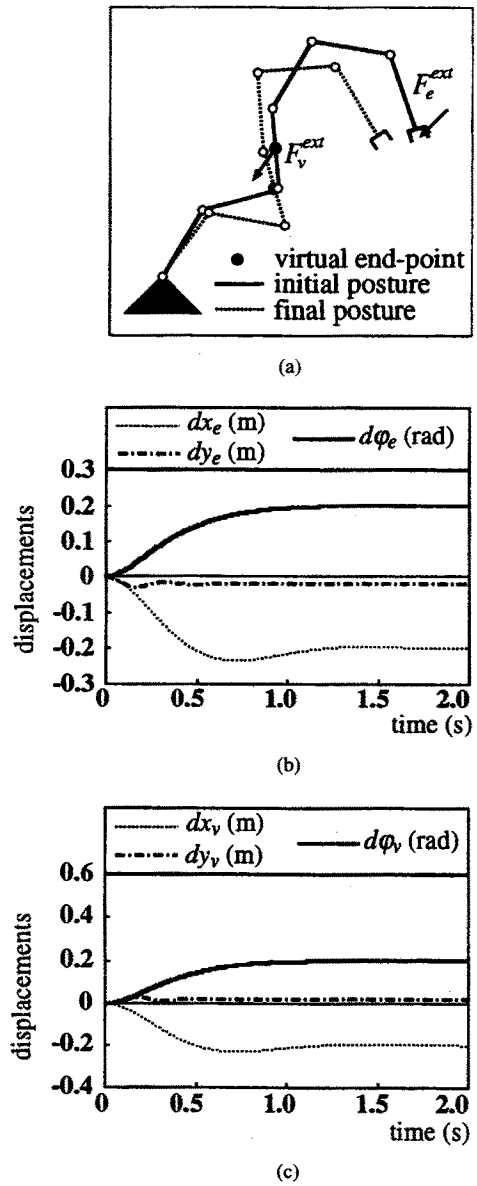

Fig. 6. Motion profile of the six-joint manipulator for external force under the first approach of the MPIC, where the virtual end-point is located on the middle of the third link: (a) stick pictures, (b) end-effector displacements, and (c) virtual end-point displacements.

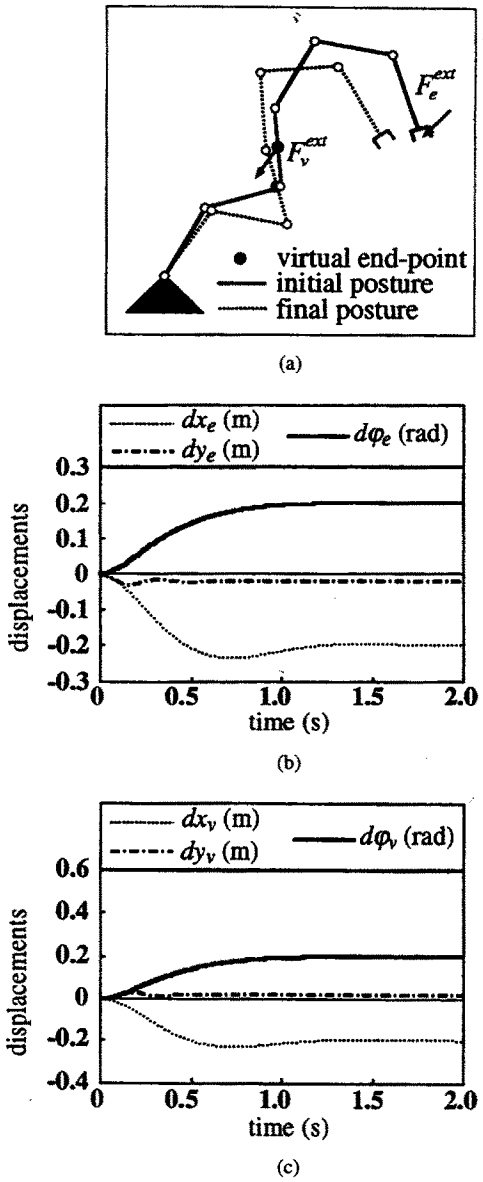

Fig. 7. Motion profile of the six-joint manipulator for external force under the second approach of the MPIC, where the virtual end-point is located on the middle of the third link: (a) stick pictures, (b) end-effector displacements, and (c) virtual end-point displacements.

of the virtual end-point are completely specified as their target impedances.

The second set of simulations is dedicated for the singular case, where the virtual end-point is located on the middle point of the fourth link of the manipulator. The desired impedances of the end-effector and the virtual end-point are the same as in the first set of the simulations. The simulation results under the first and the second approaches of the MPIC are shown in Figs. 8 and 9, respectively. As we can see from the figures, the desired multiple point impedances cannot be realized simultaneously for the singular case. Under the second approach, however, the realized end-effector impedance is exactly the same as the desired one and the virtual end-point motion is strongly reflected by its target impedance. Note that in order to avoid the internal joint motion between the virtual end-point and the base, the dissipative joint torque was added to the first and the second control laws as given by

$$\tau_{\text{dissp}} = -d\left(I_m - J_e^T \bar{J}_e^T\right) \times \left[I_m - \left\{\bar{J}_v^T\left(I_m - J_e^T \bar{J}_e^T\right)\right\}^+ \left\{\bar{J}_v^T\left(I_m - J_e^T \bar{J}_e^T\right)\right\}\right]\dot{\theta} \tag{52}$$

where $\bar{J}_v = M^{-1}J_v^T(J_v M^{-1} J_v^T)^{-1} \in \Re^{m \times n_v l}$ and $d = 10$ (Nm/(rad/s)). The dissipative joint torque is selected to act in the null space of $\bar{J}_e^T$ and $\bar{J}_v^T$, so that the following properties are guaranteed:

$$\bar{J}_e^T \tau_{\text{dissp}} = 0 \tag{53}$$

$$\bar{J}_e^T \tau_{\text{dissp}} = 0. \tag{54}$$

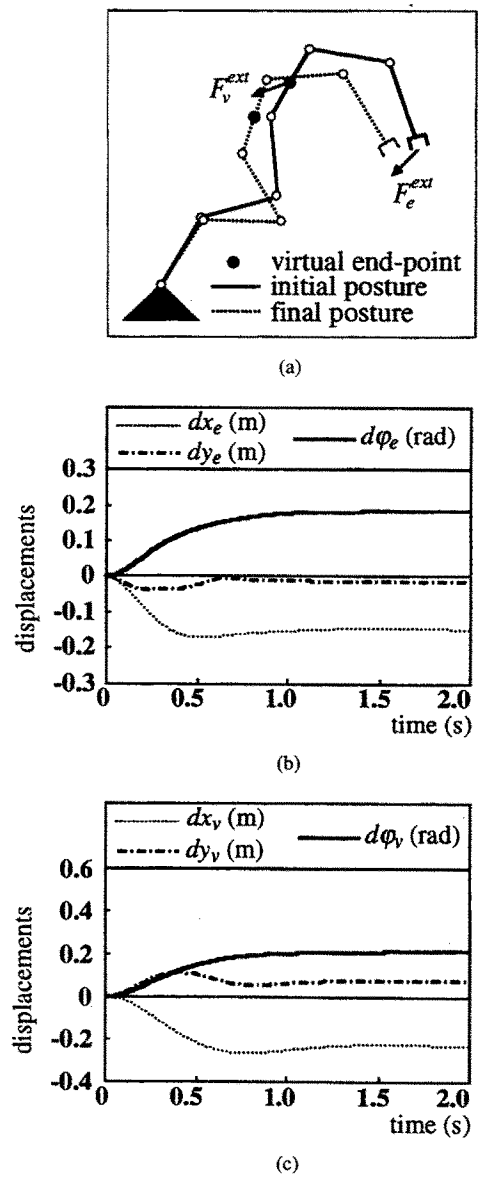

Fig. 8. Motion profile of the six-joint manipulator for external force under the first approach of the MPIC, where the virtual end-point is located on the middle of the fourth link: (a) stick pictures, (b) end-effector displacements, and (c) virtual end-point displacements.

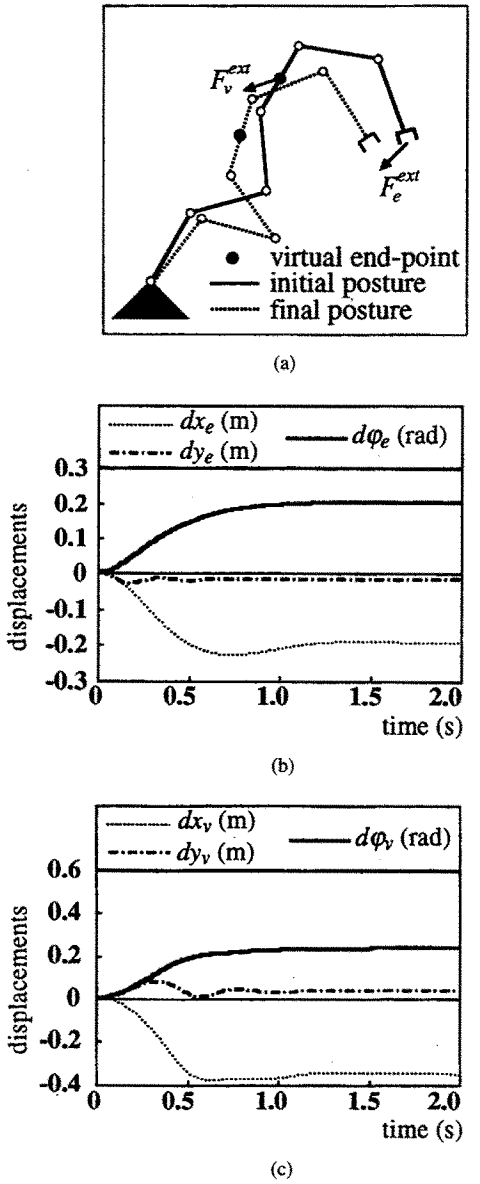

Fig. 9. Motion profile of the six-joint manipulator for external force under the second approach of the MPIC, where the virtual end-point is located on the middle of the fourth link: (a) stick pictures, (b) end-effector displacements, and (c) virtual end-point displacements.

This means that the dissipative joint torque (52) has no effect to the motion of both the end-effector and the virtual end-point.

Next, the second approach of the MPIC is applied to a three-joint planar manipulator following a circular trajectory shown in Fig. 10, and the link parameters of the manipulators are the same as in Table I. The orientation of the end-effector is arbitrary, so that the task dimension reduces to 2. Two kinds of coordinate systems are chosen as follows: 1) the world coordinate system, $\mathbf{X}(x, y)$; and 2) the polar coordinate system, $\Phi(\phi, r)$, with its origin at the center of the circle where ϕ is the rotational angle and r is the radius of the circular trajectory.

The target end-effector impedance is expressed in the polar coordinate system, where the target inertia, viscosity and stiffens matrices are given as M_e = diag. [13.5 × 10^{-3} (kgm^2), 0.2 (kg)], B_e = diag. [1.25 (Nm/(rad/s)), 20 (N/(m/s))], and K_e = diag. [31.25 (Nm/rad), 500 (N/m)], respectively. Also the desired end-effector trajectory (equilibrium trajectory) is defined as the following:

$$\begin{bmatrix} \phi_d(t) \\ r_d(t) \end{bmatrix} = \begin{bmatrix} 20\pi t^3/t_f^3 - 30\pi t^4/t_f^4 + 12\pi t^5/t_f^5 \\ r \end{bmatrix} \tag{55}$$

where the radius r and the time duration t_f are set to 0.25 m and 2.0 s, respectively. The desired velocity and acceleration of the end-effector are also obtained from (55) by differentiation.

Figs. 11 and 12 show simulation results performed under the conventional impedance control and the second approach of the MPIC, respectively. The virtual end-point was located

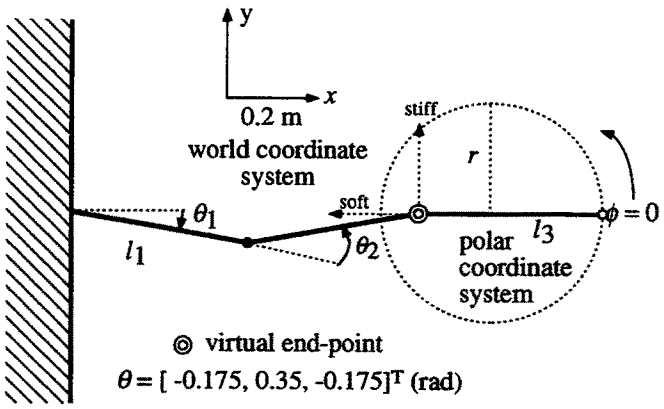

Fig. 10. Three-joint planar manipulator following a circular trajectory.

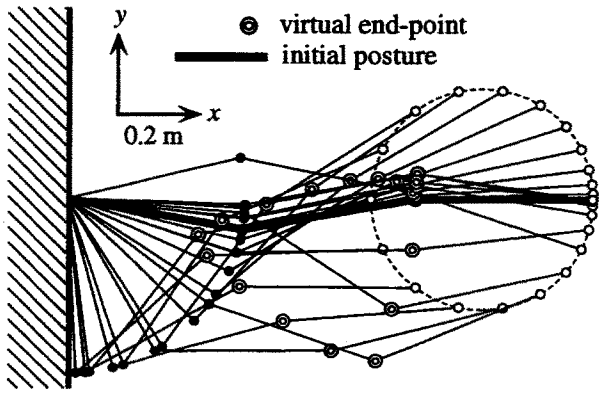

Fig. 11. Stick pictures of the three-joint planar manipulator following a circular trajectory under the conventional impedance control.

on the third joint $n_v = 1$ (see Fig. 10), and the desired virtual end-point impedance matrices are given as $M_v = \text{diag. } [0, 0.2]$ (kg), $B_v = \text{diag. } [0, 20]$ (N/(m/s)), $K_v = \text{diag. } [0, 500]$ (N/m) in respect to the world coordinate system, and the desired virtual end-point trajectory is given as $X_v^d(t) = X_v(0)$. Under these impedance matrices and the desired trajectory, the virtual end-point moves almost freely in the direction of x axis and constrained tightly in the direction of the y axis. As expected, in Fig. 12 the virtual end-point moves along the x axis during the end-effector follows the circular trajectory.

VI. Conclusion

Two approaches of the MPIC for the redundant manipulators have been proposed. The methods can regulate the impedances of several points on the links of the manipulator as well as the end-effector impedance. For the redundant cases, both approaches give the same result in which the desired impedances of the end effector and the virtual end-points can be realized exactly. The first approach provides a compact formulation and requires a simple computation for the redundant case. On the other hand, the second approach is able to regulate the impedances of virtual end-points without any effect to the end-effector motion of the manipulator, so that the desired impedance of the end-effector can be always realized.

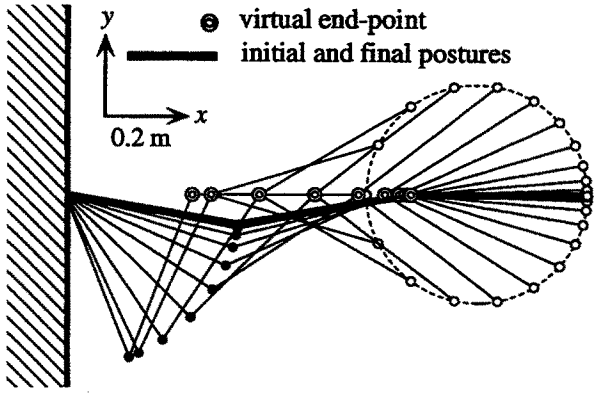

Fig. 12. Stick pictures of the three-joint planar manipulator following a circular trajectory under the second approach of the MPIC. The virtual end-point is located on the third joint of the manipulator.

Since the method requires force and acceleration measurements in the second approach, it may be limited to use in the cases where these measurements are available. It also has been assumed that the desired impedance parameters are given beforehand. Future research will be directed to develop a more practical computation technique of the MPIC and to establish the impedance planning.

Appendix A
Sufficient Condition of the HIC

Applying the control law given in (41) and (12) to the motion equation of the manipulator (40), we can find the following equation:

$$M(\theta)\ddot{\theta} = \tau_{\text{effector}} + \tau_{\text{add}} + J_e^T F_e^{\text{ext}}. \tag{A.1}$$

Now, using (6) and (A.1) and the kinematic relationships of the end-effector, we finally have

$$\tau_{\text{effector}} = J_e^T \left[\Lambda\left\{\ddot{X}_e^d - M_e^{-1}(B_e d\dot{X}_e + K_e dX_e) - \dot{J}_e\dot{\theta}\right\} - \left\{I_l - \Lambda M_e^{-1}\right\}F_e^{\text{ext}}\right] - J_e^T F_{\text{add}} \tag{A.2}$$

$$F_{\text{add}} = \Lambda J_e M^{-1}\tau_{\text{add}} \tag{A.3}$$

where $F_{\text{add}} \in \Re^l$ is the additional force on the end-effector produced by the additional joint torque, τ_{add}.

Since the additional joint torque, τ_{add}, should not produce any effect to the end-effector motion and the end-effector impedance should remain equal to the target impedance given in (6), the additional force, F_{add}, in (A.2) must be equal to zero. This yields

$$\bar{J}_e^T \tau_{\text{add}} = 0 \tag{A.4}$$

where

$$\bar{J}_e = M^{-1}J_e^T\Lambda \in \Re^{m\times l}.$$

Appendix B
Optimal Additional Controller of the HIC

Substituting (44) into (45), we find

$$G_2(z) = \left\{\tau_{\text{add}}^* - \left(I_m - J_e^T\bar{J}_e^T\right)z\right\}^T M^{-1} \times \left\{\tau_{\text{add}}^* - \left(I_m - J_e^T\bar{J}_e^T\right)z\right\}. \tag{B.1}$$

Now, the problem is how to obtain the vector z in such a way that the objective function, $G_2(z)$, is minimized. It is well known that the necessary condition regarding the optimal solution of the above problem is given by

$$\partial G_2(z)/\partial z = 0. \tag{B.2}$$

Substituting (B.1) into (B.2) and expanding it using the following properties:

$$\bar{J}_e J_e M^{-1} J_e^T \bar{J}_e^T = \bar{J}_e J_e M^{-1} = M^{-1} J_e^T \bar{J}_e^T \tag{B.3}$$

$$\left(I_m - J_e^T \bar{J}_e^T\right)^T M^{-1} = M^{-1}\left(I_m - J_e^T \bar{J}_e^T\right) \tag{B.4}$$

finally we have

$$\left(I_m - J_e^T \bar{J}_e^T\right) z = \left(I_m - J_e^T \bar{J}_e^T\right) \tau_{\text{add}}^*. \tag{B.5}$$

Then substituting (B.5) into (44), we can obtain

$$\tau_{\text{add}} = \left(I_m - J_e^T \bar{J}_e^T\right) \tau_{\text{add}}^*. \tag{B.6}$$

REFERENCES

[1] A. Liegeois, "Automatic supervisory control of the configuration and behavior of multibody mechanisms," *IEEE Trans. Syst., Man, Cybern.*, vol. SMC-7, no. 12, pp. 868–871, Dec. 1977.

[2] C. A. Klein and C. Huang, "Review of pseudoinverse control for use with kinematically redundant manipulators," *IEEE Trans. Syst., Man, Cybern.*, vol. SMC-13, no. 3, pp. 245–250, Mar./Apr. 1983.

[3] Y. Nakamura, H. Hanafusa, and T. Yoshikawa, "Task-priority based redundancy control of robot manipulators," *Int. J. Robot. Res.*, vol. 6, no. 2, pp. 3–15, 1987.

[4] T. Yoshikawa, "Analysis and control of robot manipulators with redundancy," in *Robotics Research: The First International Symposium*, M. Brady and R. Paul, Eds. Cambridge, MA: MIT Press, 1984, pp. 735–747.

[5] C. A. Klein, "Use of redundancy in the design of robotic system," in *Robotics Research: The Second International Symposium*, H. Hanafusa and H. Inoue, Eds. Cambridge, MA: MIT Press, 1985, pp. 207–214.

[6] J. Baillieul, "Avoiding obstacles and resolving kinematic redundancy," in *Proc. 1986 IEEE Int. Conf. Robot. Automat.*, 1986, pp. 1698–1704.

[7] F. T. Cheng, T. H. Chen, Y. S. Wang, and Y. Y. Sun, "Obstacle avoidance for redundant manipulators using the compact QP method," in *Proc. 1993 IEEE Int. Conf. Robot. Automat.*, 1993, pp. 262–269.

[8] O. Khatib, "Motion/force redundancy of manipulators," in *Proc. Japan-USA Symp. Flexible Automat.*, 1990, vol. 1, pp. 337–342.

[9] H. J. Kang and R. A. Freeman, "Joint torque optimization of redundant manipulators via the null space damping method," in *Proc. 1992 IEEE Int. Conf. Robot. Automat.*, 1992, pp. 520–525.

[10] T. Arai, S. H. Chiu, A. Saiki, and H. Osumi, "Proposal of dynamic redundancy in robot control," in *Proc. 1992 IEEE/RSJ Int. Conf. Intelligent Robots and Systems*, 1992, pp. 1921–1926.

[11] N. Hogan, "Impedance control: An approach to manipulation, Parts I, II, III," *ASME J. Dynamic Systems Control*, vol. 107, no. 1, pp. 1–24, 1985.

[12] ——, "Stable execution of contact tasks using impedance control," in *Proc. 1987 IEEE Int. Conf. Robot. Automat.*, 1987, pp. 1047–1054.

[13] H. Kazerooni, T. B. Shridan, and P. K. Houpt, "Robust compliance motion for manipulators, Part I: The fundamental concepts of compliant motion," *IEEE Trans. Robot. Automat.*, vol. RA-2, no. 2, pp. 83–92, June 1986.

[14] W. S. Lu and Q. H. Meng, "Impedance control with adaptation for robotic manipulation," *IEEE Trans. Robot. Automat.*, vol. 7, no. 3, pp. 408–415, June 1991.

[15] E. Colgate and N. Hogan, "An analysis of contact instability in terms of passive physical equivalents," in *Proc. 1989 IEEE Int. Conf. Robot. Automat.*, 1989, pp. 404–409.

[16] Z. W. Luo and M. Ito, "Control design of robot for compliant manipulation on dynamic environments," *IEEE Trans. Robot. Automat.*, vol. 9, no. 3, pp. 286–296, 1993.

[17] W. S. Newman and M. E. Dohring, "Augmented impedance control: An approach to compliant control of kinematically redundant manipulators," in *Proc. 1991 IEEE Int. Conf. Robot. Automat.*, 1991, pp. 30–35.

[18] Z. X. Peng and N. Adachi, "Compliant motion control of kinematically redundant manipulators," *IEEE Trans. Robot. Automat.*, vol. 9, no. 6, pp. 831–837, Dec. 1993.

[19] J. K. Salisbury, "Active stiffness control of a manipulator in cartesian coordinates," in *Proc. IEEE Conf. Decision and Control*, 1980, pp. 95–100.

[20] T. Tsuji, T. Takahashi, and K. Ito, "Multi-point compliance control for redundant manipulators," *Advances in Robot Kinematics*, S. Stifter and J. Lenaric, Eds. Vienna: Springer-Verlag, 1991, pp. 427–434.

[21] T. Tsuji, A. Jazidie, M. Kaneko, and M. Nagamachi, "Impedance control of multiple points of manipulators utilizing force redundancy," in *Proc. 3rd Int. Conf. Automat., Robot., and Computer Vision*, 1994, vol. 1, pp. 222–226.

[22] A. Jazidie, T. Tsuji, M. Kaneko, and M. Nagamachi, "Hierarchical control of end-effector impedance and joint impedance utilizing arm redundancy," in *Proc. Int. Symp. Robot Control*, 1994, vol. 2, pp. 407–412.

[23] O. Khatib, "Reduced effective inertia in macro-mini-manipulator systems," in *Proc. American Control Conf.*, 1988, pp. 2140–2147.

[24] K. Nagai and T. Yoshikawa, "Impedance control of redundant macro micro manipulators," *J. Robot. Soc. of Japan*, vol. 12, no. 5, pp. 766–772, 1994, in Japanese.

[25] T. Tsuji, S. Nakayama, and M. Ito, "Trajectory generation for redundant manipulators using virtual arms," in *Proc. 1st Int. Conf. Automat., Robot., and Computer Vision*, 1990, pp. 554–558.

[26] J. Y. S. Luh, M. W. Walker, and R. P. C. Paul, "On-line computational scheme for mechanical manipulators," *ASME J. Dynamic Systems, Measurement, and Control*, vol. 102, no. 2, pp. 69–76, 1980.

[27] M. Athan, "The Matrix Minimum Principle," *Information and Control*, vol. 11, pp. 592–606, 1967.

[28] O. Khatib, "A unified approach for motion and force control of robot manipulators: The operational space formulation," *IEEE Trans. Robot. Automat.*, vol. RA-3, no. 1, pp. 43–53, Feb. 1987.

[29] O. Egeland, J. R. Sagli, and I. Spangelo, "A damped least-squares solution to redundancy resolution," in *Proc. 1991 IEEE Int. Conf. Robot. Automat.*, 1991, pp. 945–950.

[30] D. L. Bently and K. L. Cooke, *Linear Algebra with Differential Equations*. New York: Holt, Rinehart and Winston, 1973, pp. 154–155.

[31] V. Potkonjak and M. Vukobratovic, "Two new methods for computer forming of dynamic equation of active mechanisms," *Mechanism and Machine Theory*, vol. 14, no. 3, pp. 189–200, 1979.

Toshio Tsuji was born in Kyoto, Japan, on December 25, 1959. He received the B.E. degree in industrial engineering, and the M.E. and Doctor of Engineering degrees in system engineering from Hiroshima University, Higashi-Hiroshima, Japan, in 1982, 1985, and 1989, respectively.

From 1985 to 1994, he was a Research Associate on the Faculty of Engineering at Hiroshima University, and was a Visiting Researcher at the University of Genova, Italy, from 1992 to 1993. He is currently an Associate Professor in the Industrial Engineering Department of Hiroshima University. He has been interested in various aspects of motor control in robot and human movements. His current research interests have focused on distributed planning and learning of motor coordination.

Dr. Tsuji is a member of the Japan Society of Mechanical Engineers, the Robotics Society of Japan, and the Japanese Society of Instrumentation and Control Engineers.

Achmad Jazidie received the B.S. degree in electrical engineering from Surabaya Institute of Technology (ITS), Surabaya, Indonesia, in 1984, and the M.S. degree in information engineering and Ph.D. degree in system engineering from Hiroshima University, Japan, in 1992 and 1995, respectively.

Currently, he is a Lecturer in the Electrical Department, Faculty of Industrial Technology, Surabaya Institute of Technology, Sukolilo-Surabaya, Indonesia. His main reseach interests are in kinematics, dynamics, and control of multiple and redundant manipulator systems.

Dr. Jazidie was a recipent of graduate fellowships from the Hitachi Scholarship Foundation from 1989 to 1995.

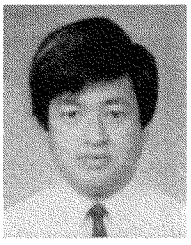

Makoto Kaneko (M'87) received the B.S. degree in mechanical engineering from Kyushu Institute of Technology, Fukuoka, Japan, in 1976, and the M.S. and Ph.D. degrees in mechanical engineering from Tokyo University, Japan, in 1978 and 1981, respectively.

From 1981 to 1990, he was a Researcher at the Mechanical Engineering Laboratory (MEL), Ministry of International Trade and Industry (MITI), Tsukuba Science City, Japan. From 1988 to 1989, he was a Post-Doctoral Fellow at Technical University of Darmstadt, Germany, where he joined a space robotics project. From 1990 to 1993, he was an Associate Professor with Computer Science and System Engineering, Kyushu Institute of Technology. From November 1991 to January 1992, he obtained an Invited Professorship at Technical University of Darmstadt, Germany. Since October 1993, he has been a Professor in the Industrial Engineering Department at Hiroshima University, Higashi-Hiroshima, Japan. His research interests include tactile-based active sensing, grasping strategy, sensor applications, and experimental robotics.

Dr. Kaneko received the Outstanding Young Engineer Award in 1983 from the Japan Society of Mechanical Engineers. He also received the Outstanding Paper Award from the Robotics Society of Japan in 1994. He served as a Technical Editor of IEEE TRANSACTIONS ON ROBOTICS AND AUTOMATION from 1990 through 1994. He has been a Program Committee member for IEEE International Conference on Intelligent Robots and Systems since 1991. He worked as a Program Committee member for the 1995 IEEE International Conference on Robotics and Automation. He is also a member of the Japan Society of Mechanical Engineers, the Robotics Society of Japan, and the Japanese Society of Instrumentation and Control Engineers.